Deterministic dynamics of neural activity during absence seizures in rats

Gaoxiang Ouyang,[1] Xiaoli Li,[2,*] Chuangyin Dang,[1] and Douglas A. Richards[3]
[1]*Department of MEEM, City University of Hong Kong, Kowloon, Hong Kong*
[2]*Institute of Electrical Engineering, Yanshan University, Qinhuangdao 066004, China*
[3]*Department of Pharmacology, School of Clinical and Experimental Medicine, College of Medical and Dental Sciences, The University of Birmingham, Birmingham B15 2TT, United Kingdom*
(Received 25 October 2008; revised manuscript received 19 February 2009; published 29 April 2009)

The study of brain electrical activities in terms of deterministic nonlinear dynamics has recently received much attention. Forbidden ordinal patterns (FOP) is a recently proposed method to investigate the determinism of a dynamical system through the analysis of intrinsic ordinal properties of a nonstationary time series. The advantages of this method in comparison to others include simplicity and low complexity in computation without further model assumptions. In this paper, the FOP of the EEG series of genetic absence epilepsy rats from Strasbourg was examined to demonstrate evidence of deterministic dynamics during epileptic states. Experiments showed that the number of FOP of the EEG series grew significantly from an interictal to an ictal state via a preictal state. These findings indicated that the deterministic dynamics of neural networks increased significantly in the transition from the interictal to the ictal states and also suggested that the FOP measures of the EEG series could be considered as a predictor of absence seizures.

DOI: 10.1103/PhysRevE.79.041146 PACS number(s): 05.40.−a, 05.45.Tp, 87.19.xm, 87.19.le

I. INTRODUCTION

Absence epilepsy, in which the seizures are accompanied by spike-and-wave complexes, is a form of brain disorder initiated by abnormally discharging neurons that recruit and entrain neighboring neurons into a critical mass [1,2] and is associated with significant changes in the EEG series [3,4]. Recently, several methods have been developed to analyze the temporal evolution of epileptic seizure of the brain from the EEG series [5,6]. These methods range from the traditional linear analysis, such as Fourier transforms and spectral analysis [7], to nonlinear analysis derived from the theory of nonlinear dynamical systems (also called chaos theory), such as the Lyapunov exponents [8,9] and correlation dimension [10–12]. To some extent, these chaos-based methods are capable of extracting informative features from epileptic EEG data [5,8,11] and are superior to the traditional linear methods [13]. In reality, a real epileptic EEG is a nonstationary signal and stems from a highly nonlinear system [14]. Therefore, applications of chaos-based methods to analyzing epileptic EEG data are still limited [15,16].

Recently, Bandt and Pompe [17,18] introduced permutation entropy as a computationally fast and conceptually simple measure for the irregularity of a nonstationary time series that does not require a reconstruction of an attractor in state space. The basic principle of this method is consideration of the order relations between the values of a time series and not the values themselves, and as a result, it is robust in the presence of observational and dynamical noise [17,19]. Moreover, another advantage of the Bandt-Pompe method is that it can discover a fundamental distinction between deterministic chaos and noisy systems [20,21]. These advantages facilitate the use of methods based on the Bandt-Pompe algorithm for investigating the intrinsic ordinal structures in complex time series, such as in physical systems [19–33], physiological systems [18,34–40], and in engineering [41,42].

The Bandt-Pompe-method-based forbidden ordinal patterns (FOP) has been developed to evaluate the determinism of a given time series [23–25]. For a sufficiently long random time series, all ordinal patterns will appear, and therefore no pattern is forbidden. For a time series with deterministic behaviors, some patterns would not be encountered due to the underlying deterministic structure, and these are called *forbidden ordinal pattern* [23,42]. It has been demonstrated that most chaotic systems exhibit FOP, and that in many cases the measure of the number of these patterns is related to other classical metric entropy rates (e.g., the Lyapunov exponent) [22,23]. These properties can be embodied in a simple method to distinguish deterministic from random events [23]. In this paper, we investigated the existence of FOP in the EEG series in a rat model of absence epilepsy. Specifically, we investigated whether or not the FOP measures of the EEG series could effectively distinguish the preictal state from the interictal and ictal states in order to evaluate whether FOP measures could be used to predict absence seizures in this rat model of absence epilepsy.

II. MATERIALS AND METHODS

A. Animal experiments and EEG series

All procedures were performed under a British Home Office project license [UK Animals (Scientific Procedures) Act, 1986]. Experiments were performed in 24 male genetic absence epilepsy rats from Strasbourg (GAERS) of at least 13 weeks of age. At this stage of development, all GAERS display the characteristic repeated spike-wave discharges (SWDs) on the EEG [43] during absence seizure. They were anesthetized with medetomidine/ketamine (0.5 and 75 mg/kg i.p., respectively) for the duration of the surgery, with imme-

*Corresponding author. xiaoli.avh@gmail.com

diate postoperative reversal of the effects of medetomidine with atipamezole (1 mg/kg s.c.). In all animals, a bipolar twisted-wire EEG electrode (MS303/1; Semat Technical, St. Albans, UK) was implanted in the frontal cortex (mm, relative to bregma; AP, 2.2: L, 2.4: V, 2.6 from the dura mater). The headmounts were secured to two skull screws with dental cement (Duralay II), and the animals were allowed to recover overnight with free access to water and rat diet. The following day, after connection of a cable to the EEG electrode, the animal was transferred to an EEG recording cage and left to acclimatize to this environment for at least 45 min. The signal from the EEG electrode was directly visualized on an oscilloscope and was further amplified (BioAmp ML 136), filtered, digitized (100 Hz), and stored using a POWERLAB 2/20 RUNNING CHART v4.2 software (ADInstruments, Hastings, UK). Once regular SWD were being observed, 30 min of EEG was recorded from each animal. The EEG data sets were preprocessed by a 50 Hz notch filter and a high pass filter at 0.5 Hz.

B. Visual inspection of the EEG series

The EEGs were visually inspected by an experienced experimental scientist to define the interictal EEG activities, seizure, and artifacts. In all rats, the interictal EEG were normal. The onset and offset of absence seizures were determined by the start and end times of SWDs, and these SWDs were defined as large-amplitude rhythmic 7–8 Hz discharges with typical spike-wave morphology lasting >1.0 s. Intervals containing major artifacts were excluded from the analysis. Start and end times for all SWDs were marked. Individual absence seizures in GAERS ranged from 3 to 71 s in duration with an average length of 19.6 s. From all seizures recorded, those where the time gap between seizure onset and the offset of the previous seizure was less than 30 s were excluded from further analysis. Using these criteria, the total length of seizures recorded was 8.4 h, with an average total duration of 21 min per rat (range: 15–24 min), and this comprised a total of 251 absence seizures (range: 5–15 per rat) in 24 rats.

C. Ordinal patterns

Ordinal patterns analysis is a technique of evaluating the dynamic characteristics of a given time series [17,26]. Given a time series of length L, $\{x_1,x_2,\ldots,x_L\}$, a vector can be generated by an embedding procedure: $S_t=[x_t,x_{t+\tau},\ldots,x_{t+(m-1)\tau}]$, where m and τ are the embedding dimension and the lag, respectively. This vector S_t can be rearranged in an ascending order, $[x_{t+(j_1-1)\tau}\leq x_{t+(j_2-1)\tau}\leq\cdots\leq x_{t+(j_m-1)\tau}]$. To obtain a unique result, we set $j_{r-1}<j_r$ in the case of $x_{t+(j_{r-1}-1)\tau}=x_{t+(j_r-1)\tau}$. For m different numbers, there will be $m!=(1\times2\times\cdots\times m)$ possible ordinal patterns π_i, $i=m!$, also called permutations. For example, for $m=3$, there are six ordinal patterns among x_t, $x_{t+\tau}$, and $x_{t+2\tau}$ as shown in Fig. 1(a), and the relation $x_{t+2\tau}<x_t<x_{t+\tau}$ corresponds to the ordinal pattern $\pi_4=231$. Figure 1(b) illustrates the ordinal patterns of a white-noise time series (left) and the logistic map (right) [$x_{n+1}=4x_n(1-x_n)$ and $0<x_0<1$], with $m=3$ and

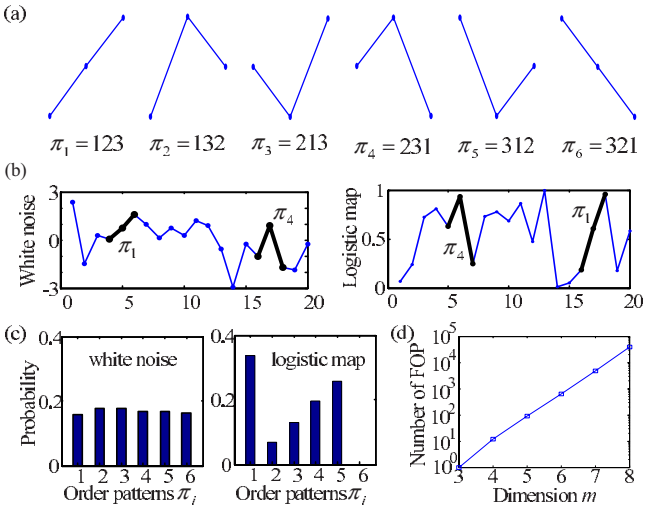

FIG. 1. (Color online) Ordinal patterns in simple time series. (a) The six ordinal patterns of the dimension $m=3$. (b) Illustration of the ordinal procedure for $m=3$ and $\tau=1$ for white-noise and logistic map time series. (c) Probability distribution of order pattern π_i. (d) The number of FOP in the logistic map time series ($L=10^6$) are computed with different dimensions, $m=\{3,4,5,6,7,8\}$.

$\tau=1$. Then we can count the occurrences of the ordinal pattern π_i, which is denoted as $C(\pi_i)$, and the relative frequency is calculated by $p(\pi_i)=C(\pi_i)/[L-(m-1)\tau]$, $i=1,2,\ldots,m!$, as can be seen in Fig. 1(c).

D. Forbidden ordinal patterns

As shown in Fig. 1(c), the distributions of ordinal patterns of the white-noise and logistic map time series are quite different. With regard the white-noise time series, all ordinal patterns appear (i.e., no patterns are forbidden) because of the characteristics of random behavior, and the probability distribution of the ordinal patterns is even. In contrast, with the logistic map time series, the pattern of $\pi_6=321$ disappears because of characteristics of deterministic behavior, called forbidden ordinal pattern [23]. Furthermore, if an ordinal pattern of dimension m is "forbidden," its absence pervades all longer dimensions of m in the form of more missing ordinal patterns [24]. As shown in Fig. 1(d), the number of FOP of the logistic map time series grows superexponentially with the length of dimension m.

Most chaotic systems exhibit FOP, and in many cases the measure of the number of these patterns is related to other classic metric entropy rates (e.g., the Lyapunov exponent) [22,23]. In other words, the existence of FOP should be a hallmark of deterministic orbit generation and it can be used to discriminate deterministic from random systems [24]. However, when FOP analysis is applied to real-time series, the finiteness of sequences will produce *false FOP* (i.e., ordinal patterns are missing in a random sequence without constraints). Thus, the application of this method requires some attention since real-time series are *finite* (making it possible that random sequences have false FOP with finite probability) and *noisy* (blurring the difference between determinism and randomness) [25]. To this end, a sufficiently long series

is required to avoid producing false forbidden patterns. Given the embedding dimension m and the lag τ and a time series of length L, the number of possible ordinal patterns is $m!$, while the number of groups of data is $L-(m-1)\tau$. To ensure all possible ordinal pattern of dimension m occur in a time series of length L, the condition $L-(m-1)\tau \geq m!$ must be satisfied. For this reason, given a dimension of length m, we need to choose $L \geq (m+1)!$.

E. FOP analysis of EEG series

A crucial parameter in the forbidden orbital patterns estimation is the choice of the embedding dimension m for analysis of EEG recordings. When m is too small (less than 3), there are only very few distinct states for the EEG series; a larger value of m would be better for a long EEG series. In this study, too large a value of m would be inappropriate to investigate ordinal pattern characteristics of the EEG series of absence seizures since the average duration of each seizure is 19.6 s (less than 2000 samples). Therefore, to satisfy the condition of $L \geq (m+1)!$, we chose a low dimension $m=4$ or $m=5$ and delay $\tau=1$ for the FOP analysis in this study.

To illustrate the effect of parameter choice on the estimation of FOP, an example is shown in Fig. 2. Figure 2(a) plots a long-term EEG series of 180 s during a period of the interictal state. A moving window technique was applied to obtain the FOP from the EEG series. The criteria of windows overlapped were that the time distance between two consecutive windows was 0.1 s (10 samples). The number of FOP, $n(4,L)$, in each EEG segment is shown for the moving window of length 120 samples with overlap of 110 samples [Fig. 2(b)], the moving window of length 160 samples with overlap of 150 samples [Fig. 2(c)], and the moving window of length 200 samples with overlap of 190 samples [Fig. 2(d)]. It was observed that the FOP occur most frequently in the window of length 120 samples and occur least frequently in the window of length 200 samples. To observe the FOP in EEG segments of different window lengths L, we counted the total number of FOP $\Sigma n(m,L)$ for $(m+1)! \leq L \leq 2000$ in a long-term EEG recording, as shown in Fig. 2(e) for dimensions $m=4$ and $m=5$. It was found that the number of FOP decayed with increasing length L in an EEG recording. This is because the greater the value of L, the more unlikely that a dimension m pattern is missing in a noisy or random time series of length L [23,24,42].

F. Testing the significance

In this study, a surrogate data method [44] was used to test the significance for FOP detection in EEG series. The null hypothesis is taken to be that the time series data represents the Gaussian linear stochastic processes and not nonlinear processes. We generated surrogate time series by using a Fourier transform of the original EEG series followed by the inverse Fourier transform with phase randomization [45,46]. In the surrogate data, the autocorrelation of the original EEG data, i.e., the underlying linear autoregressive processes, is preserved, while the nonlinear determinism included in the original data, if any, has been lost. Hence, a significant difference in the statistics between the original and the surrogate data indicates that the null hypothesis should be rejected and that nonlinear determinism is likely to be present in the original data.

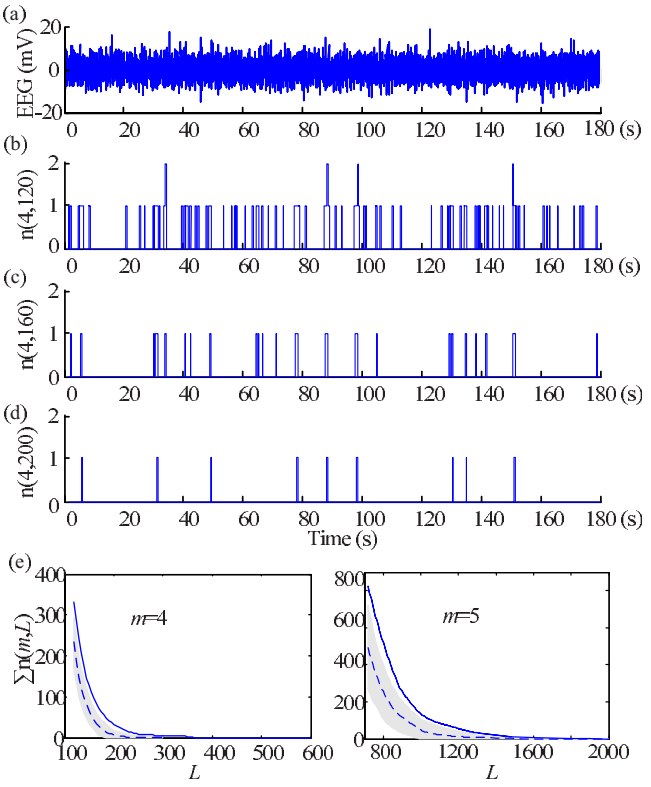

FIG. 2. (Color online) The FOP in the interictal EEG recording. (a) A representative example of a long-term interictal EEG series from GAERS. The EEG series were spilt into overlapping segments by a moving window technique. The time profile of the number of FOP (dimension $m=4$) in each EEG segment for: (b) the moving window of length 120 samples with overlaps of 110 samples, (c) the moving window of length 160 samples with overlaps of 150 samples, and (d) the moving window of length 200 samples with overlaps of 190 samples. (e) The total number of FOP $\Sigma n(m,L)$ in this long-term EEG recording for dimensions $m=4$ (left) and $m=5$ (right). The dashed lines represent the mean values of $\Sigma n(m,L)$ and the gray shadow represents the 95% confidence interval for the surrogate data method (see statistical analysis below).

The number of FOP was calculated for surrogate time series generated from original EEG recordings. If determinism in the original EEG series is significant, the average number of FOP in the surrogate data, $\langle n(m,L)\rangle_{\text{sur}}$, will be smaller than that in the original EEG data, $\langle n(m,L)\rangle_{\text{EEG}}$. To test for a statistically "significant difference" (Theiler's sigma) [44] in average number of FOP between original and surrogate data, 100 surrogate data series are generated to match each original EEG signal. Let $\langle n(m,L)\rangle^i_{\text{sur}}$ be the average number of FOP of 100 surrogate series $(i=1,2,\ldots,100)$. If the difference between the original and the surrogate $\langle n(m,L)\rangle$ is significantly larger than the standard deviation of the surrogate $\langle n(m,L)\rangle$, then this is a strong indication of the deterministic structure in the investigated EEG recordings. The mean and standard deviation of $\langle n(m,L)\rangle^i_{\text{sur}}$ are estimated as $\overline{\langle n(m,L)\rangle_{\text{sur}}}$ and $\text{SD}[\langle n(m,L)\rangle^i_{\text{sur}}]$. Theiler's sigma is then computed by

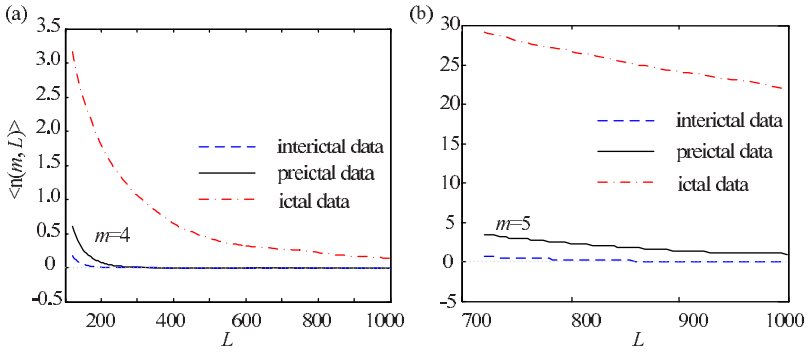

FIG. 3. (Color online) Average number of FOP of dimension m found in EEG epochs of length L, $\langle n(m,L)\rangle$, for interictal data (dashed line), preictal data (solid line), and ictal data (dot-dashed line), which gradually increases from the interictal to the ictal state for dimensions (a) $m=4$ and (b) $m=5$, respectively.

$$[\langle n(m,L)\rangle_{\mathrm{EEG}} - \overline{\langle n(m,L)\rangle_{\mathrm{sur}}}]/\mathrm{SD}[\langle n(m,L)\rangle^{i}_{\mathrm{sur}}]. \quad (1)$$

This statistic represents the number of standard deviations distant from $\langle n(m,L)\rangle_{\mathrm{EEG}}$ and approximately follows a normal distribution. For $\alpha=0.05$, the critical value is 1.96. Accordingly, when Theiler's sigma is above 1.96, the null hypothesis is rejected at the 95% probability level [46].

III. RESULTS

A. Forbidden ordinal patterns in EEG series

To investigate whether forbidden ordinal patterns were present in the EEG series, 93 seizures were first extracted from GAERS EEG data. The criteria for the selection of the seizure EEG data were that the intervals between the end and beginning points of seizures were greater than 50 s and that the duration of seizure was greater than 10 s. Then, the EEG series were dissected from the interictal state (starting 10 s after the end point of previous seizure and ending 10 s before the beginning point of seizure), the preictal state (starting 10 s before the beginning point of seizure and ending the beginning point of seizure), and the ictal state (starting the beginning point of seizure and ending 10 s after the beginning point of seizure). Thus, longer (50 s and more) interictal epochs, 10 s preictal epochs, and 10 s ictal epochs were obtained for each of the 93 seizures. Previous studies had shown that the duration of the preictal state was only around a few seconds as determined by using entropy [39] or synchronization measures [3].

Figure 2 is an example of FOP measures in a representative interictal EEG recording. As shown in Fig. 2(e), we counted the total number of FOP $\Sigma n(m,L)$ for a $(m+1)! \le L \le 2000$ long-term EEG recording and its surrogate data. Calculating the total FOP in the surrogate data sets with the moving window technique, the range within which 95% of false FOPs fell was illustrated by the gray shadow areas [see Fig. 2(e)]. The results showed that the phase randomized surrogate data sets produced false FOP due only to statistical limitations and that their number diminished to zero with increasing length of the time series. Comparing the surrogate data sets and the original EEG series, there were more missing ordinal patterns in the EEG series, and the number of FOP significantly decreased with the sample length, L.

The above procedure was used to process all 279 EEG epochs (3×93). To compare the number of FOP in EEG epochs during different states, we calculated the average number of FOP $\langle n(m,L)\rangle$ for $(m+1)! \le L \le 1000$ in the interictal, preictal, and ictal EEG epochs respectively, as shown in Fig. 3. The results showed that the number of FOP within ictal EEG epochs was much higher than that in interictal EEG epochs. The average number of FOP with different windows length, L, gradually increased from the interictal to ictal states for dimensions $m=4$ and $m=5$, respectively.

The numbers of FOP were also calculated for the surrogate time series generated from each EEG epoch. With dimension $m=4$ and window length $L=120$, the mean and standard deviations of FOP in the interictal, preictal, and ictal EEG epochs were 0.173 ± 0.024 (range 0.129–0.210), 0.591 ± 0.139 (range 0.279–0.912), and 3.172 ± 1.407 (range 0.494–5.988), while in the corresponding surrogated series were 0.131 ± 0.018 (range 0.101–0.175), 0.372 ± 0.156 (range 0.142–0.912), and 1.062 ± 0.684 (range 0.154–3.030), respectively. The average number of FOP computed on the surrogate data, $\overline{\langle n(4,120)\rangle_{\mathrm{sur}}}$, versus the average number of FOP of the corresponding original EEG data, $\langle n(4,120)\rangle_{\mathrm{EEG}}$ is plotted in Fig. 4. From Fig. 4, it can be seen that most data points (+) are distributed below the line $\overline{\langle n(4,120)\rangle_{\mathrm{sur}}} = \langle n(4,120)\rangle_{\mathrm{EEG}}$, so the average number of FOP in the original EEG data is significantly greater than in the surrogate data ($P<0.05$, Wilcoxon rank sum test) during the interictal, preictal, and ictal phases, respectively. As a further check of nonlinearity, the value of "Theiler's sigma" was computed for each EEG epoch. The Theiler's sigma values in the interictal, preictal, and ictal intervals are plotted in Fig. 5, and the average of these values are 1.76 ± 1.62, 3.06 ± 2.86, and 9.96 ± 5.94 (mean $\pm$ SD), respectively. Using the surrogate technique to determine whether a significant difference exists in the number of FOP between original and surrogate data, the results show that evidence for nonlinearity in EEG epochs in the interictal, preictal, and ictal intervals are present in 41 of 93 (44.1%), 56 of 93 (60.2%), and 86 of 93 (92.5%) of seizures, respectively.

B. Prediction of absence seizures

Next we considered whether the FOP method could be considered as predictive of absence seizures in GAERS. In this part of the study, a moving window technique (window length of 1.2 s with an overlap of 1.1 s) was applied to calculate the FOP number of the EEG series. The criterion of windows overlapped was that the time distance between two consecutive windows was 0.1 s (10 samples). For the prediction of absence seizures, only the lower dimension $m=4$ was

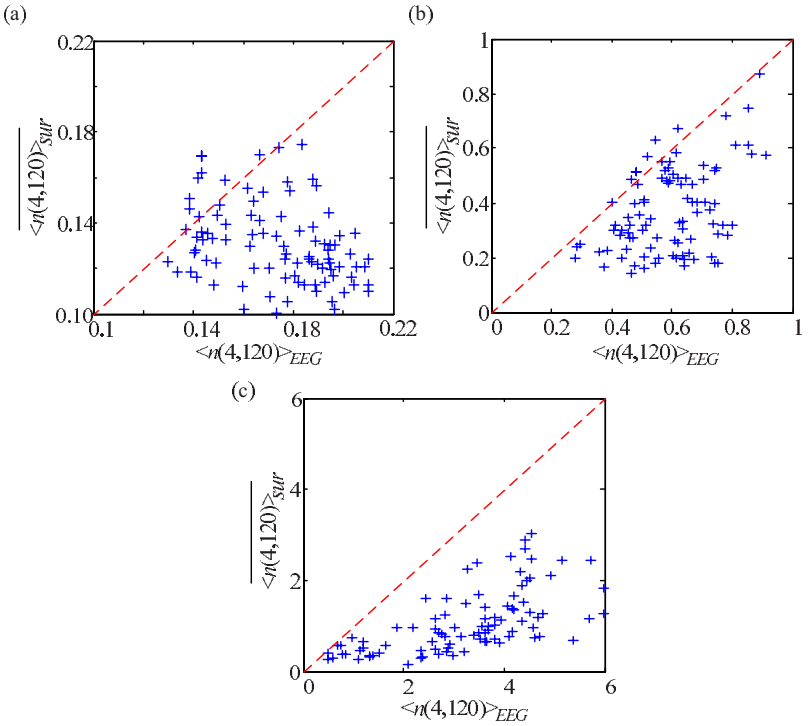

FIG. 4. (Color online) Comparison of the *average number of FOP* in original EEG data, $\langle n(4,120)\rangle_{\mathrm{EEG}}$, with the mean FOP in the corresponding set of 100 surrogates, $\langle n(4,120)\rangle_{\mathrm{sur}}$. Each dot (plus sign) corresponds to a 10 s EEG segment in the (a) interictal, (b) preictal, and (c) ictal intervals in GAERS. Data points under the dashed straight line represent the number of FOP in EEG data larger than surrogates and vice versa.

selected during the calculation of FOP. This was because (i) the dimension m must satisfy the condition of $(m+1)!<L$ and (ii) the duration of the preictal state is only around a few seconds as determined by using entropy [39] or synchronization measures [3]. Figure 6(a) shows an EEG series including two absence seizures. At time $t=60$ s, an absence seizure occurred. The definitions of interictal, preictal, and ictal states are as described above, i.e., that the interval between the interictal EEG segments and the end and beginning points of seizures is greater than 10 s. The relative frequency $p(\pi_i)$ of order patterns in each EEG segment for dimension $m=4$ is shown in Fig. 6(b). Different relative frequency distributions of EEG segments during different seizure states can be seen. In particular, during the ictal state, the repeated SWD is a characteristic of absence epilepsy so that the num-

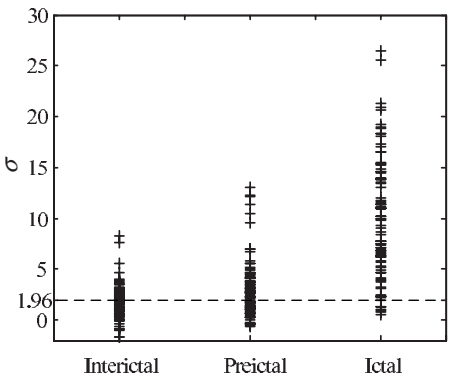

FIG. 5. Theiler's sigma of FOP in EEG data in the interictal, preictal, and ictal intervals. The signal value can test the significance of difference in the number of FOP between the original and surrogate EEG data. The statistical value of Theiler's sigma approximately follows a normal distribution, so for $a=0.05$, the critical value is 1.96.

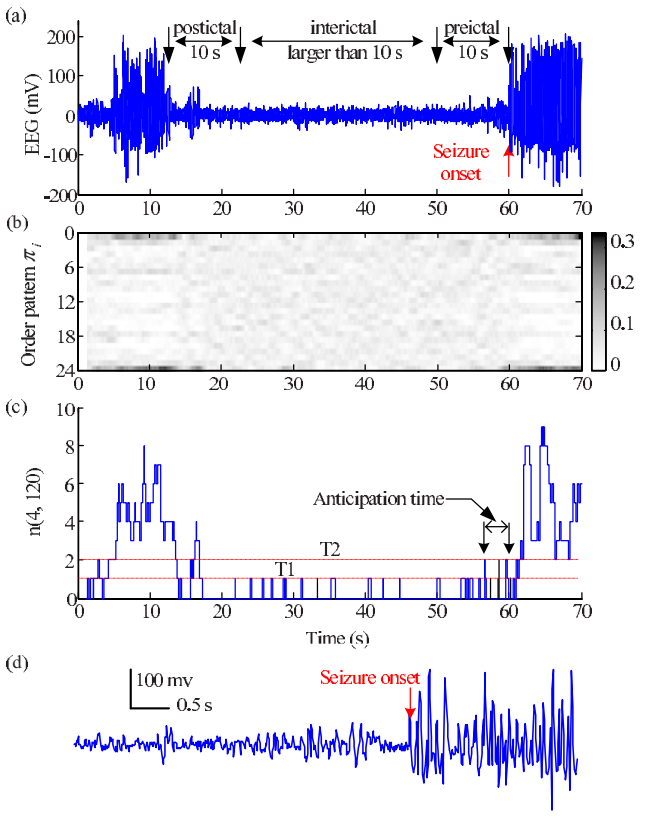

FIG. 6. (Color online) The prediction analysis of absence seizures from EEG series. (a) The continuous EEG series with two seizures. (b) The relative frequency $p(\pi_i)$ of order patterns have been obtained using a moving window technique and are shown in a color scale, indicating the actual value from the smallest in white to the largest in black. (c) The time profile of the number of FOP in each EEG segment. (d) The zoomed seizure onset.

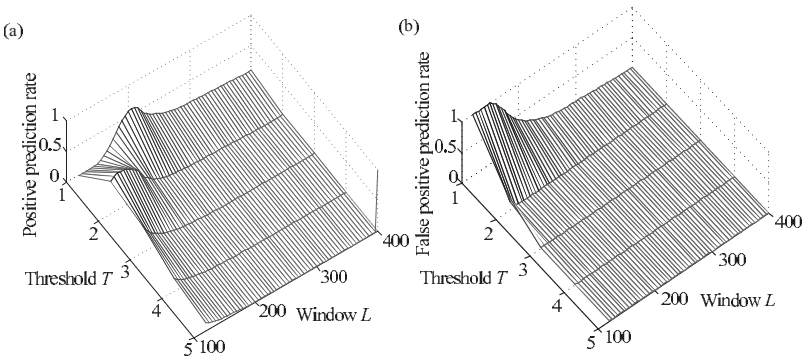

FIG. 7. The results of seizure prediction in the entire 251 absence seizures with different window lengths L and thresholds T. The (a) positive predictions and (b) false positive predictions are represented with a three-dimensional mesh plot.

ber of FOP in the EEG segments increases markedly from the interictal state to the ictal state, as shown in Fig. 6(c). During the interictal state only the number of FOP $n(4,120)=1$ is present. However, during the preictal state (starting 10 s prior to seizure onset) the number of FOP $n(4,120)=2$ is observed for some EEG segments.

Next, to investigate the predictability of absence seizures with order patterns analysis, the number of FOP was applied to detect the preictal state. The threshold, T, for detecting preictal state, was determined by the number of FOP $n(m,L)$ in EEG segments. The cross point between $n(m,L)$ and the threshold T is called a precursor; and the interval between the precursor and the onset of the seizure was defined as the anticipation time in this study. As illustrated in Fig. 6(c), when the threshold $T_2=2$ was selected, the preictal state was successfully detected, defined as a *positive prediction*, at time $t=55.5$ s, i.e., the anticipation time was 4.5 s. When the threshold $T_1=1$ was chosen, the anticipation time larger than 10 s, i.e., the preictal state was falsely detected during the interictal phase, and this is called a *false positive prediction.* When the threshold T was greater than 2, no alarm was obtained during the preictal and interictal states, meaning that this threshold could not successfully predict this absence seizure. On lowering the threshold further, the seizure prediction method becomes not only more sensitive in the preictal phase, but eventually also in the interictal state, leading to more false positive predictions [47]. The above method (window length $L=120$ and dimension $m=4$) was applied to analyze the entire EEG data set. With threshold $T=2$, from 251 seizures, the FOP measures can find that 50.2% of the seizures contain predictive states; 17.9% of the seizures do not. The false positive rate of this detection method is 31.9%.

To further investigate the performance of this prediction method, it was applied to the entire data set with different window lengths L (varying from 120 to 400 with a step of five samples) and thresholds T (varying from 1 to 5 with a step of 1). As shown in Fig. 7, it was found that the number of false positive predictions decreased with the increase in threshold value T, and there were no false positive predictions in all 251 absence seizures when the threshold value T was equal to or greater than 4. On the other hand, the number of false positive predictions gradually decreased with the increase in the window length L. This is because the number of FOP in EEG generally decreased with the length of a noisy EEG segment. Additionally, this seizure prediction method was robust in the interictal state when the value of threshold T or window L is big but reduced the positive prediction rates in the preictal state. In this study, the largest number of positive predictions, 155 out of 251 seizures (61.8%), was obtained with the parameters of threshold $T=2$ and window length $L=130$. However, for the same threshold and window length, there was also a relatively high false positive prediction rate (11 out of 251). The practicalities of seizure prediction are that false positive predictions cannot entirely be prevented. However, too many false alarms may result in a negative effect on the patients who may not take further alarms seriously and may thus be unprepared for a seizure. On the other hand, those epilepsy patients who take all alarms seriously may suffer from huge psychological stress as a result of false positives. Thus, a seizure prediction method should obtain as high a positive prediction rate and as low a false positive prediction rate as possible [47]. With the parameters of threshold $T=2$ and window length $L=140$, we obtained the best performance of prediction with positive prediction in 151 out of 251 seizures (60.2%) and only a single false positive prediction.

IV. DISCUSSION

The theory of nonlinear dynamical systems has provided the basis for a method of studying pattern formation in the complex neuronal networks of the brain. An established method is to reconstruct a phase space from the EEG series then and then to characterize the dynamics of brain activity in terms of its dimension or its Lyapunov exponents and entropy [5]. Recently, methods have been developed to characterize other features of local brain dynamics, including forecasting, time asymmetry and determinism [5]. In this study, the FOP method has been presented for analyzing the determinism of EEG series in GAERS. This has revealed a high number of FOPs during the ictal state that is greater than during the interictal state. Thus, the determinism (regularity) of the EEG series could be applied to predict oncoming absence seizures.

A. Determinism in EEG series

In this study, the extracellular recording of local-field potentials (LFPs) in the frontal cortex was analyzed. These recordings represent a running average of all of the dendritic activities surrounding the implanted electrode. In particular, the oscillatory properties of LFPs can be observed, such as the spike-wave discharges that characterize the absence seizure state, which are related to activity in the functional

structures of the neural network. Most neuronal networks are nonlinear excitable systems. Therefore, an important issue is to answer the question of whether neural networks display deterministic behavior or are purely stochastic [48].

In this study, a high number of FOPs in the EEG series during the ictal state were found, which indicates that the determinism of the EEG series is significant during absence seizures (see Fig. 3). Similar results have been reported previously. For example, in [4], a recurrence quantification analysis was applied to indicate the deterministic dynamics of the EEG series at the seizure-free, preseizure, and seizure states in GAERS. The results showed that EEG epochs during preseizure intervals exhibited a higher degree of determinism than during seizure-free EEG epochs but lower than those in seizure EEG epochs in absence epilepsy. In [49], Cao's method and the differential entropy method were used to estimate the embedding dimensions of normal and epileptic EEG series, and it was shown that epileptic EEG signals have determinism. By characterizing the trajectories of the EEG signals via singular value decomposition, the determinism for intracranial EEG recordings during seizures was more significant than during nonseizures [50]. These findings support the belief that the underlying dynamics of EEG series in absence epilepsy is related to their increased determinism (regularity), arising from the synchronous discharge of large numbers of neurons [1,2].

Furthermore, we have used the surrogate data method to test the significance level of FOP measures, and to discriminate deterministic dynamics from a random series (see Figs. 4 and 5). The number of FOPs in the original EEG data during the interictal state was significantly greater than those in the surrogate data. It was also found that the Theiler's sigma value of greater than 1.96 was presented in 41 of 93 (44.1%) in the interictal EEG series. This result is consistent with the fact that EEG signals contain complex structures across multiple spatial and temporal scales. These results support the view that EEG signals are not random but contain complex deterministic structural information [13,51,52]. However, the determinism is not significantly detected in the remaining 52 interictal EEG series. The absence of nonlinearity, or the failure to detect nonlinearity, could be related to the fact that EEG series are noisy. It suggests that these EEGs within interictal intervals are generated by a high-dimensional process that cannot be distinguished from noise on the basis of these analyses [53,54]. Therefore, a further study will be needed to reconfirm the nonlinearity in the interictal EEG series by using another surrogate method.

It was observed that the number of FOP in preictal EEG epochs was higher than that in interictal EEG epochs but lower than that in ictal EEG epochs. A possible reason for this is that the epileptic process induces or enhances nonlinear deterministic structures in an otherwise linear stochastic appearance of the EEG [4,55,56]. The absence seizure is initiated by abnormally discharging neurons that recruit and entrain neighboring neurons into a critical mass. This process manifests itself as increasing synchronization of neuronal activity [1,2], which implies an increasing determinism of the EEG data. These results are similar to the findings that different EEG rhythms were presented in different pathological brain states [6,52].

B. Prediction of absence seizures

Over the past ten years, many strategies for analyzing and predicting seizures have been evaluated, including linear and nonlinear measures, such as the Lyapunov exponents [8,9], correlation dimension [10–12], similarity [57,58], and other methods [59,60]. However, since the EEG data include the transient signal embedded in noise and nonstationary signals [14], the detection of the evolutionary characteristics of EEG data is still an open issue [15,16], and the existing prediction methods are still not sufficiently robust for clinical applications [6]. It is thus desirable to develop new prediction methods for epileptic seizures.

Our results showed that the FOP measure could provide a quantitative value to differentiate interictal, preictal, and ictal states based on the ordinal dynamics patterns in EEG series, which led us to investigate whether or not the FOP measures could be effectively used to predict absence seizures (see Figs. 5 and 6). Analysis of the entire EEG data found that FOP measures successfully predicted absence seizures prior to the onset in 151 out of 251 seizures (60.2%) with the threshold value of $T=2$. During absence seizures, the firing pattern of the thalamocortical neurons shifts to an oscillatory rhythmic synchronized state of the EEG [61]. Recent evidence, however, has suggested a focal initiation site for absence seizures within the facial somatosensory cortex [62–64], which can then recruit and entrain neighboring cortical and thalamic neurons into a critical mass, i.e., an increasing synchronization of neuronal activity. In this study, we can also observe there is an increase in signal amplitude and regularity before appearance of the first spike and wave component [see Fig. 6(d)], and this is a major reason of the increasing number of FOP during the preictal state.

Furthermore, another important advantage of the FOP method to predict epileptic seizures is the very simple algorithm and hence faster computation: (i) only three parameters: dimension m, window length L, and threshold T, need to be selected; and (ii) the FOP measure of a single channel EEG of 1.5 s could be calculated in less than 2 ms by using MATLAB (Math Works Inc.) on a 1.6 GHz personal computer. In comparison to the prediction of seizures with permutation entropy and sample entropy [39], FOP measures are better able to predict absence seizures. Therefore a real-time online seizure prediction can be obtained based on FOP measures. These results suggest that FOP measures in the EEG data have the potential of providing the basis for designing an automated closed-loop seizure prevention system for absence epilepsy. An important next goal will be to confirm the results presented here in a large clinical cohort of absence epilepsy patients.

ACKNOWLEDGMENTS

The valuable comments and suggestions from the anonymous reviewers to improve this work were appreciated. This research was supported by Program for New Century Excellent Talents in University (Grant No. NECT-07-0735), National Natural Science Foundation of China (Grant No. 90820016), and Strategic Research Grant of City University of Hong Kong (Grant No. 7002224).

[1] H. K. Meeren, J. P. Pijn, E. L. Van Luijtelaar, A. M. Coenen, and F. H. Lopes da Silva, J. Neurosci. **22**, 1480 (2002).
[2] P. O. Polack, I. Guillemain, E. Hu, C. Deransart, A. Depaulis, and S. Charpier, J. Neurosci. **27**, 6590 (2007).
[3] A. Aarabi, F. Wallois, and R. Grebe, Brain Res. **1188**, 207 (2008).
[4] G. X. Ouyang, X. L. Li, C. Y. Dang, and D. A. Richards, Clin. Neurophysiol. **119**, 1747 (2008).
[5] C. J. Stam, Clin. Neurophysiol. **116**, 2266 (2005).
[6] W. C. Stacey and B. Litt, Nat. Clin. Pract. Neurol. **4**, 190 (2008).
[7] Z. Rogowski, I. Gath, and E. Bental, Biol. Cybern. **42**, 9 (1981).
[8] L. D. Iasemidis, J. Sackellares, H. Zaveri, and W. Williams, Brain Topogr. **2**, 187 (1990).
[9] L. D. Iasemidis and J. Sackellares, Neuroscientist **2**, 118 (1996).
[10] R. G. Andrzejak, K. Lehnertz, F. Mormann, C. Rieke, P. David, and C. E. Elger, Phys. Rev. E **64**, 061907 (2001).
[11] C. E. Elger and K. Lehnertz, Eur. J. Neurosci. **10**, 786 (1998).
[12] K. Lehnertz and C. Elger, Phys. Rev. Lett. **80**, 5019 (1998).
[13] M. I. Rabinovich, P. Varona, A. I. Selverston, and H. D. I. Abarbanel, Rev. Mod. Phys. **78**, 1213 (2006).
[14] D. Gribkov and V. Gribkova, Phys. Rev. E **61**, 6538 (2000).
[15] R. Aschenbrenner-Scheibe, T. Maiwald, M. Winterhalder, H. U. Voss, J. Timmer, and A. Schulze-Bonhage, Brain **126**, 2616 (2003).
[16] Y. C. Lai, Mary Ann F. Harrison, M. G. Frei, and I. Osorio, Phys. Rev. Lett. **91**, 068102 (2003).
[17] C. Bandt and B. Pompe, Phys. Rev. Lett. **88**, 174102 (2002).
[18] M. Staniek and K. Lehnertz, Int. J. Bifurcation Chaos Appl. Sci. Eng. **17**, 3729 (2007).
[19] O. A. Rosso, L. Zunino, D. G. Perez, A. Figliola, H. A. Larrondo, M. Garavaglia, M. T. Martin, and A. Plastino, Phys. Rev. E **76**, 061114 (2007).
[20] J. M. Amigo and M. B. Kennel, Physica D **231**, 137 (2007).
[21] O. A. Rosso, H. A. Larrondo, M. T. Martin, A. Plastino, and M. A. Fuentes, Phys. Rev. Lett. **99**, 154102 (2007).
[22] J. M. Amigo, M. B. Kennel, and L. Kocarev, Physica D **210**, 77 (2005).
[23] J. M. Amigo, S. Zambrano, and M. A. F. Sanjuan, EPL **79**, 50001 (2007).
[24] J. M. Amigo, S. Elizalde, and M. B. Kennel, J. Comb. Theory, Ser. A **115**, 485 (2008).
[25] J. M. Amigo and M. Kennel, Physica D **237**, 2893 (2008).
[26] C. Bandt, G. Keller, and B. Pompe, Nonlinearity **15**, 1595 (2002).
[27] C. Bandt, Ecol. Modell. **182**, 229 (2005).
[28] C. Bandt and F. Shiha, J. Time Ser. Anal. **28**, 646 (2007).
[29] K. Keller and K. Wittfeld, Int. J. Bifurcation Chaos Appl. Sci. Eng. **14**, 693 (2004).
[30] K. Keller and M. Sinn, Physica A **356**, 114 (2005).
[31] K. Keller, M. Sinn, and J. Emonds, Stochastics Dyn. **7**, 247 (2007).
[32] A. Bahraminasab, F. Ghasemi, A. Stefanovska, P. V. E. McClintock, and H. Kantz, Phys. Rev. Lett. **100**, 084101 (2008).
[33] L. Zunino, D. G. Pérez, M. T. Martín, M. Garavaglia, A. Plastino, and O. A. Rosso, Phys. Lett. A **372**, 4768 (2008).
[34] A. A. Bruzzo, B. Gesierich, M. Santi, C. A. Tassinari, N. Birbaumer, and G. Rubboli, Neurol. Sci. **29**, 3 (2008).
[35] Y. H. Cao, W. W. Tung, and J. B. Gao, Phys. Rev. E **70**, 046217 (2004).
[36] B. Frank, B. Pompe, U. Schneider, and D. Hoyer, Med. Biol. Eng. Comput. **44**, 179 (2006).
[37] A. Groth, Phys. Rev. E **72**, 046220 (2005).
[38] K. Keller, H. Lauffer, and M. Sinn, Chaos Complexity Lett. **2**, 247 (2007).
[39] X. L. Li, G. X. Ouyang, and D. A. Richards, Epilepsy Res. **77**, 70 (2007).
[40] X. L. Li, S. Y. Cui, and L. Voss, Anesthesiology **109**, 448 (2008).
[41] X. L. Li, G. X. Ouyang, and Z. H. Liang, Int. J. Mach. Tools Manuf. **48**, 371 (2008).
[42] M. Zanin, Chaos **18**, 013119 (2008).
[43] L. Danober, C. Deransart, A. Depaulis, M. Vergnes, and C. Marescaux, Prog. Neurobiol. **55**, 27 (1998).
[44] J. Theiler, S. Eubank, A. Longtin, B. Galrikian, and J. Farmer, Physica D **58**, 77 (1992).
[45] T. Schreiber and A. Schmitz, Phys. Rev. Lett. **77**, 635 (1996).
[46] T. Schreiber and A. Schmitz, Physica D **142**, 346 (2000).
[47] M. Winterhalder, T. Maiwald, H. U. Voss, R. Aschenbrenner-Scheibe, J. Timmer, and A. Schulze-Bonhagea, Epilepsy Behav. **4**, 318 (2003).
[48] M. W. Slutzky, P. Cvitanovic, and D. J. Mogul, J. Neurosci. Methods **118**, 153 (2002).
[49] Y. Yuan, Y. Li, D. P. Mandic, and A. Comparison, J. Physiol. Sci. **58**, 239 (2008).
[50] A. H. Meghdadi, R. Fazel-Rezai, and Y. Aghakhani, *Conference Proceeding of the IEEE Engineering in Medicine and Biology Society 2007, Lyon, France*, 2007, pp. 2008–2011.
[51] N. Burioka, G. Cornelissen, Y. Maegaki, F. Halberg, D. T. Kaplan, M. Miyata, Y. Fukuoka, M. Endo, H. Suyama, Y. Tomita, and E. Shimizu, Clin. EEG Neurosci. **36**, 188 (2005).
[52] G. Buzsaki, *Rhythms of the Brain* (Oxford University Press, Oxford, 2006).
[53] K. J. Blinowsk and M. Malinowski, Biol. Cybern. **66**, 159 (1991).
[54] J. Theiler and P. E. Rapp, Electroencephalogr. Clin. Neurophysiol. **98**, 213 (1996).
[55] R. G. Andrzejak, F. Mormann, G. Widman, T. Kreuz, C. E. Elger, and K. Lehnertz, Epilepsy Res. **69**, 30 (2006).
[56] X. L. Li, D. Cui, P. Jiruska, J. E. Fox, X. Yao, and J. G. Jefferys, J. Neurophysiol. **98**, 3341 (2007).
[57] M. Le Van Quyen, J. Martinerie, M. Baulac, and F. Varela, NeuroReport **10**, 2149 (1999).
[58] G. X. Ouyang, X. L. Li, Y. Li, and X. P. Guan, Comput. Biol. Med. **37**, 430 (2007).
[59] K. Lehnertz and B. Litt, Clin. Neurophysiol. **116**, 493 (2005).
[60] F. Mormann, R. G. Andrzejak, C. E. Elger, and K. Lehnertz, Brain **130**, 314 (2007).
[61] M. Steriade, D. A. McCormick, and T. J. Sejnowski, Science **262**, 679 (1993).
[62] H. K. Meeren, J. P. Pijn, E. L. Van Luijtelaar, A. M. Coenen, and F. H. Lopes da Silva, J. Neurosci. **22**, 1480 (2002).
[63] H. Meeren, G. van Luijtelaar, F. H. Lopes da Silva, and A. Coenen, Arch. Neurol. **62**, 371 (2005).
[64] P. O. Polack, I. Guillemain, E. Hu, C. Deransart, A. Depaulis, and S. Charpier, J. Neurosci. **27**, 6590 (2007).